DELETION OF CONNEXIN43 IN OSTEOBLASTS/OSTEOCYTES LEADS TO IMPAIRED MUSCLE FORMATION IN MICE

- SUPPLEMENTAL DOCUMENT -

Hua Shen, MD, PhD[1]

Susan Grimston, PhD[2]

Roberto Civitelli, MD[1,2]

Stavros Thomopoulos, PhD,[1]

[1]Department of Orthopaedic Surgery, Washington University, St. Louis, MO, USA
[2]Division of Bone and Mineral Disease, Department of Internal Medicine, Washington University, St. Louis, MO, USA

Address correspondence to: Stavros Thomopoulos, PhD, Department of Orthopaedic Surgery, Washington University, 660 South Euclid Avenue, Campus Box 8233, St. Louis, MO 63110, USA. Phone: 314-362-8605. Email address: thomopouloss@wudosis.wustl.edu

Supplemental Results

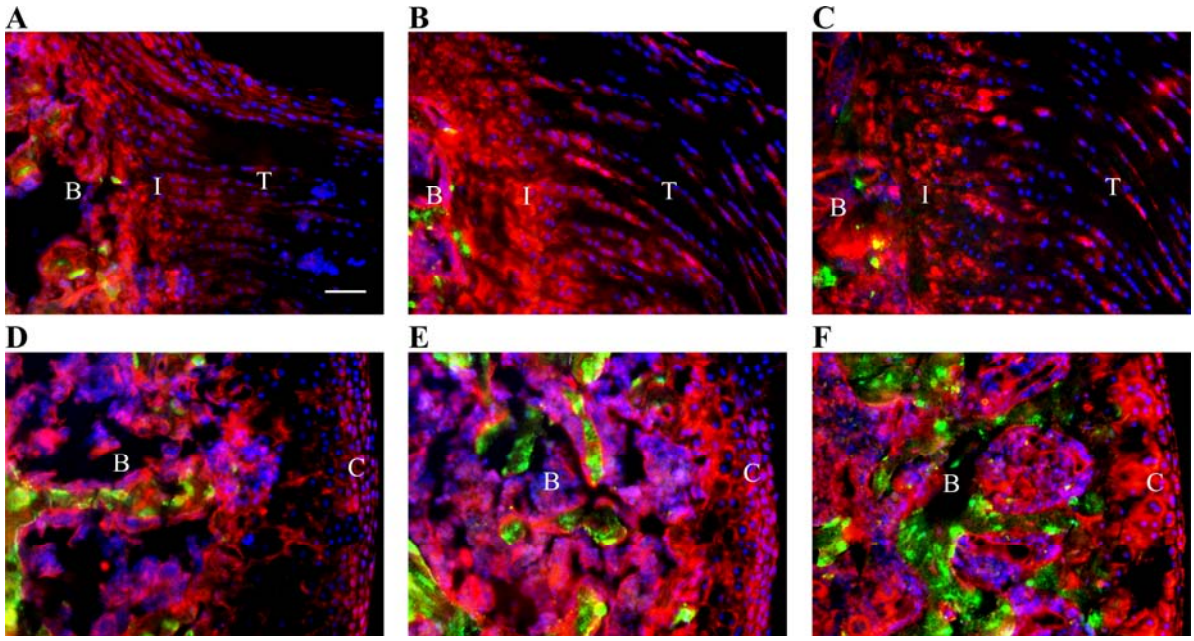

Supplemental Fig. 1. Expression of Col1Cre in mouse shoulder. **A** - **F**, Representative fluorescence images of SS tendon with its humeral head insertion (**A - C**) and proximal humeral head (**D - F**) from coronal sections of P14 (**A** and **D**), P28 (**B** and **E**), and P56 (**C** and **F**) *Col1Cre;mTmG* mouse shoulders. Col1Cre expression (in green) was detected in OCYs /OBs in humeral bone (B) but not in SS tendon (T), non-bone region of SS tendon-to-bone insertion (I), and humeral head cartilage (C) counterstained with DAPI (in blue). Bar, 50 μm.

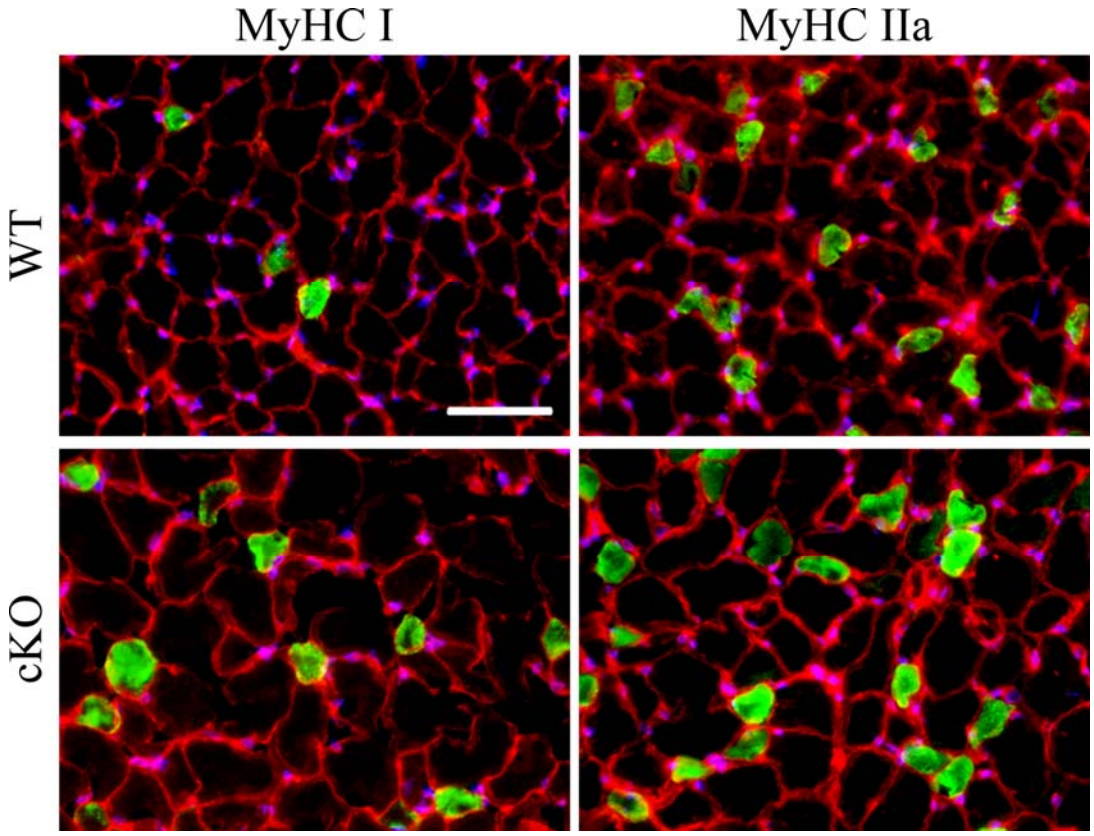

Supplemental Fig. 2. Representative images for the expression of myosin heavy chain type I (MyHC I) and type IIa (MyHC IIa) fibers in P28 extensor digitorum longus (EDL) muscles. Mouse EDL muscles were stained with antibodies specific for either MyHC I (green in the left panels) or MyHC IIa (green in the right panels), wheat germ agglutinin (WGA; in red for muscle fiber boundaries), and Bisbenzimide H33258 (in blue for cell nuclei). Bar, 50 μm.

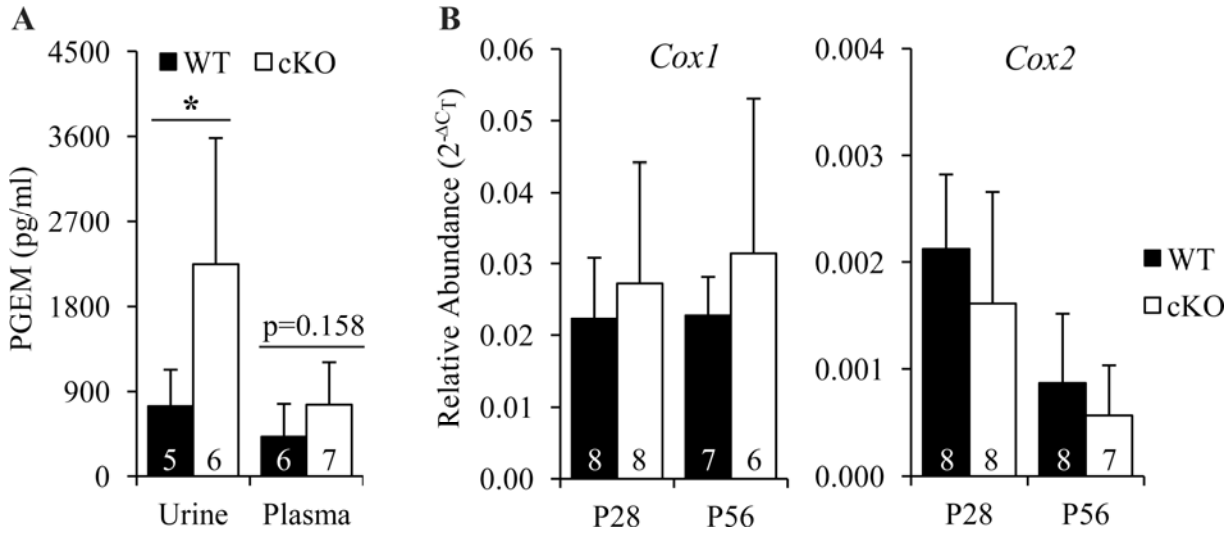

Supplemental Fig. 3. Cx43 deficiency in osteoblasts (OBs)/osteocytes (OCYs) was accompanied with an increase in systemic prostaglandin E2 (PGE2). **A**, Urine and plasma prostaglandin E metabolites (PGEMs) from P28 mice were detected by an enzyme immunoassay. *, $p = 0.039$, t-test. **B**, Relative abundances of *Cox1* and *Cox2* mRNA in humeri of WT and *Gja1* cKO mice were evaluated by quantitative realtime RT-PCR. $p = 0.212$ and 0.146 for the effect of genotype on *Cox1* and *Cox2* expression, 2-way ANOVA, Sample sizes are indicated at the bottom of each column.

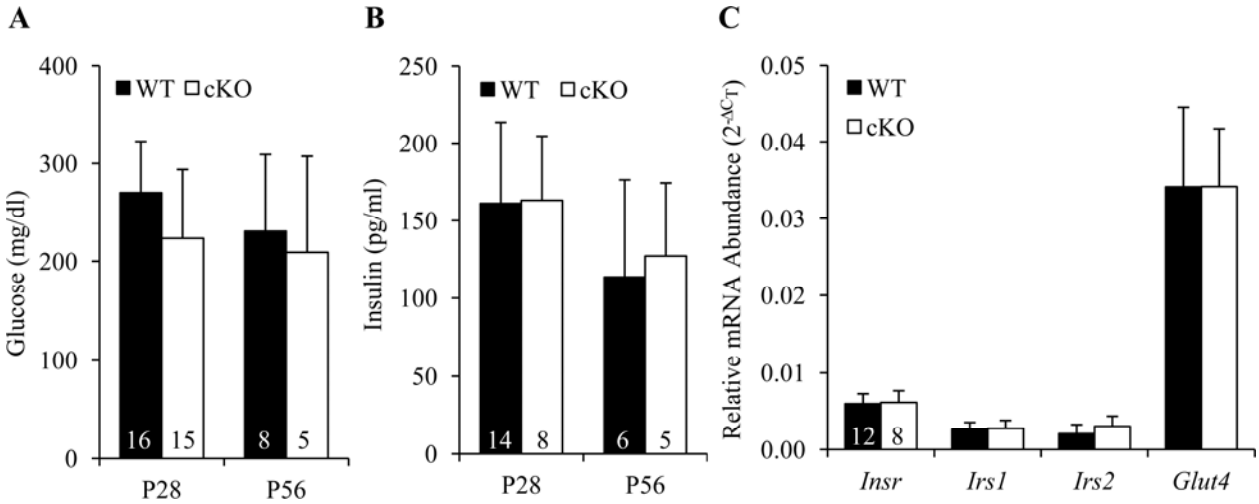

Supplemental Fig. 4. The effect of Cx43 deficiency in OBs/OCYs on blood insulin and glucose levels and the expression of genes involved in muscle insulin signaling and glucose transport. **A** and **B**, Blood glucose (A) and insulin (B) levels in WT and *Gja1* cKO mice after 5 – 6 h morning fast. $p > 0.05$ between WT and cKO for both A and B, 2-way ANOVA. Sample sizes are indicated at the bottom of each column. **C**, Relative mRNA abundance of genes encoding insulin receptor (*Insr*), insulin receptor substrate 1 and 2 (*Irs1* and *Irs2*) and glucose transporter (*Glut4*) in P28 SS muscle from WT and *Gja1* cKO mice. $p > 0.05$, WT vs. cKO, t-test. Sample sizes are indicated on the first two columns from the left.

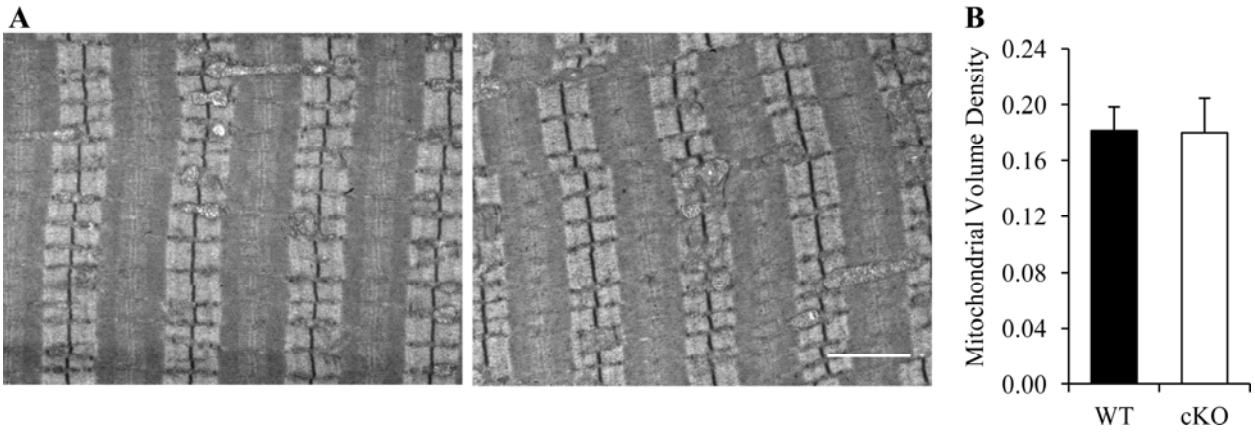

Supplemental Fig. 5. Representative transmission electron microscopy images (**A**) and quantification (**B**) for mitochondrial volume density from EDL muscle of P28 WT (left panel) and cKO (middle panel) mice. Bar, 2 µm. $p = 0.827$, WT vs. cKO, t-test.

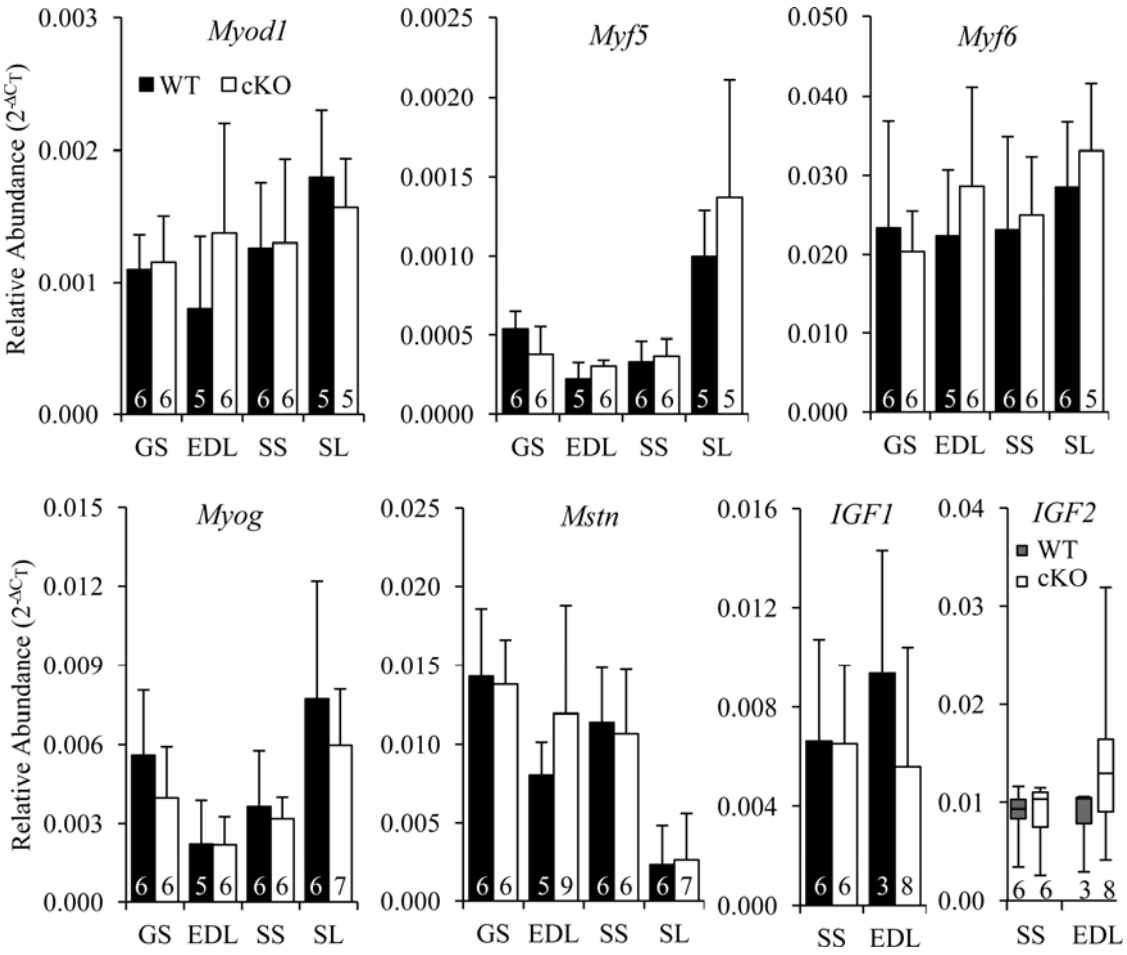

Supplemental Fig. 6. Cx43 deficiency in OBs/OCYs does not alter mRNA abundance of gene products involved in myogenesis and muscle growth in P28 mouse muscles. Abundance of mRNA was determined by quantitative realtime RT-PCR. Sample sizes are indicated at the bottom of each column/box. $p > 0.05$ for all comparisons between WT and cKO; t-test was used for all but IGF2 analyses, for which Mann-Whitney rank sum test was performed.

Supplemental Tab. 1. Trabecular bone indexes at the humeral head of WT and *Gja1* cKO mice.

	P14		P28		P56	
Index	WT (N=8)	cKO (N=12)	WT (N=7)	cKO (N=9)	WT (N=7)	cKO (N=15)
BV/TV (%)[a]	14.36±5.30	15.49±3.21	28.34±3.37	28.46±3.72	32.90±4.84	32.07±5.30
Tb.N[b]	44.00±17.60	39.07±18.15	13.99±0.46	14.11±5.36	14.65±0.53	14.35±0.41
Tb.Th (mm)[c]	0.024±0.003	0.025±0.006	0.037±0.003	0.037±0.003	0.054±0.005	0.054±0.005
Tb.Sp (mm)[d]	0.037±0.011	0.036±.019	0.075±0.003	0.073±0.004	0.086±0.002	0.083±0.003

[a], bone volume fraction; [b], trabecular number; [c], trabecular thickness; [d], trabecular space.

Supplemental Materials and Methods

Glucose, insulin, and PGE2 assay. All mice were fasted for 5h to 6 h prior to blood withdrawal. Mouse urine and plasma prostaglandin E2 levels were determined using Prostaglandin E Metabolite EIA Kit (Cayman Chemical). Plasma glucose and insulin measurements were performed with Autokit Glucose (Wako Diagnostics) and Erenna Immunoassay System (Singulex) at Washington University Diabetes Research Center and Core Laboratory for Clinical Studies, respectively.

Muscle force measurement. GS muscle was dissected while animal was under isoflurane anesthesia. Each muscle was tied with silk sutures (6-0) at the proximal end of the Achilles tendon and its attachment site to the distal end of the femur. The muscle was positioned between electrodes (Radnoti Glass Technology) in a tissue bath (Radnoti Glass Technology) filled with Ringer's lactate solution at 22-24ºC and attached to FT03 force transducer (Grass Technologies) at its distal end with sutures. The muscle was stimulated with an S48 square wave pulse stimulator (Grass Technologies). Muscle contractile force was recorded via a FT03 force transducer connected to a P11T amplifier (Grass Technologies). Care was given during dissection to avoid direct contact with the muscles to be tested. The integrity of each muscle included in this study was verified prior to and after muscle force measurement,

Transmission electron microscopy and muscle mitochondrial volume density. EDL muscles from P28 mice were freshly dissected (N=3 per group), pinned on cork at its natural length, and fixed in 2% paraformaldehyde/2.5% glutaraldehyde in 100 mM phosphate buffer (pH 7.2) for 1 hr at room temperature. After 1 h postfix in 1% osmium tetroxide (Polysciences Inc.) and 1 h en bloc staining with 1% aqueous uranyl acetate (Ted Pella Inc., Redding, CA), tissues were dehydrated in a graded series of ethanol and embedded in Eponate 12 resin (Ted Pella Inc.). Longitudinal sections of 95 nm were cut with a Leica Ultracut UCT ultramicrotome (Leica Microsystems Inc.), stained with uranyl acetate and lead citrate, and viewed on a JEOL 1200 EX transmission electron microscope (JEOL USA Inc.) equipped with an AMT 8 megapixel digital camera (Advanced Microscopy Techniques.). Five fibers per sample were imaged. For each fiber, three images were taken at 6000 × magnification (corresponding to an area of 11 µm x 8.5 µm) at three predefined regions: R1, right under nucleus, R2, on the left side of R1, R3, on the right side of R1. Thus, total 15 images were obtained from each sample. Mitochondrial volume density (Vd_{mito}) were determined using a stereological point counting method.[1] Specifically, each image was superimposed with 513 nm × 513 mm grids in Photoshop CS5.1. The number of points (intersection of two grid lines) that touched mitochondria (P_{mito}) were tallied and divided by the total number of point on the grid (P_{total}), which is equal to 374. The Vd_{mito} for each sample is the average of P_{mito}/P_{total} from all 15 images.

Supplemental References

1. Broskey NT, Daraspe J, Humbel BM, Amati F. Skeletal muscle mitochondrial and lipid droplet content assessed with standardized grid sizes for stereology. J Appl Physiol. 2013;115:765-70.